Science Arts & Métiers (SAM)
is an open access repository that collects the work of Arts et Métiers Institute of Technology researchers and makes it freely available over the web where possible.

This is an author-deposited version published in: https://sam.ensam.eu
Handle ID: .http://hdl.handle.net/10985/18695

To cite this version :

P. NGUYEN-TRI, Cyrille SOLLOGOUB, Alain GUINAULT - Relationship between fiber chemical treatment and properties of recycled pp/bamboo fiber composites - Journal of Reinforced Plastics and Composites - Vol. 29, n°21, p.3244-3256 - 2010

Any correspondence concerning this service should be sent to the repository Administrator : scienceouverte@ensam.eu

Relationship between fiber chemical treatment and properties of recycled pp/bamboo fiber composites

Nguyen Tri Phuong, Cyrille Sollogoub and Alain Guinault

Abstract

This article reports the preparation of recycled polypropylene (RPP)/bamboo fiber (BF) composite via direct melt blends using a twin screw extruder. The effects of the chemical treatment of BF surface (alkaline and acetylation) on fiber structure and composite mechanical, thermal, rheological properties have been investigated. We showed that alkali treatment increases the contact surface of BF within composites, resulting in a more homogenous dispersion of fibers in the polymer matrix. Alkali treatment improves mechanical properties such as tensile strength as well as the Charpy impact strength. Reinforced composites obtained with acetylated BF show better mechanical properties due to grafting of acetyl groups onto the cellulose fiber surface and thus improve compatibility between BF and matrix. The rheological properties of RPP/BF composites depending on the BF content and treatment methods are also analyzed. Predominant factors that influence the properties of relevant materials are identified. Maleic anhydride grafted polypropylene is used as a compatibilizer to improve the adhesion between the cellulosic phase and the RPP matrix.

Keywords

Adhesion, bamboo fibers, recycled polypropylene, rheological behavior

Introduction

Synthetic fiber-reinforced polymer composites have many applications, such as use in automotive, construction, aerospace, and sports equipment. Glass fibers are mainly used because of their low cost, easy production processing, and relatively high mechanical properties. However, the problems encountered in the use of these materials originate in their negative impact on the environment and also their potential adverse effects when used in contact with humans (skin allergies, lung cancer, etc.). Specific regulations that restrict the use of these products are in existence. In contrast, the use of vegetable fibers has always been encouraged due to their many advantages, including their abundant availability, their renewable nature, and sometimes facile degradation.[1] They are also lighter, cheaper, and show acceptable properties. Their production requires lower energy and for many applications it may be advantageous to use vegetable fibers in place of glass fibers to reinforce polymers.

Today, a wide range of natural fibers can be used in order to improve the performance of polymers. Many thermoplastic polymers may be chosen as the matrix of polymer/vegetable fiber composites, such as polyethylene (PE),[2,3] polypropylene (PP),[4,5] polystyrene (PS),[6,7] and polyvinylchloride (PVC).[8,9] These polymers show good properties when reinforced by vegetable fibers. Their cost is low and they can be processed at medium temperatures (under 220°C) thus avoiding thermal degradation of vegetable fibers.

Like other perennial grasses, bamboo grows particularly well in tropical and subtropical countries. According to a recent report,[1] there are about 60–70 genera and over 1250 species of bamboo in the world, of which half grow in Asia. Bamboos have been widely used in diverse applications from domestic products to

Conservatoire National des Arts et Métiers (CNAM), 292 rue Saint Martin, 75003 Paris, France.

Corresponding author:
Cyrille Sollogoub, Conservatoire National des Arts et Métiers (CNAM), 292 rue Saint Martin, 75003 Paris, France
Email: cyrille.sollogoub@cnam.fr

industrial uses such as furniture, flooring, musical instruments, textile, handicrafts, containers, toys, and scaffolding. Bamboo is a fast growing species and a highly renewable resource. Some bamboo species can reach maximum height in 4–6 months with a daily increment of 15–18 cm.[10] The potential use of bamboo fibers (BF) as reinforcement for composite materials has focused the increasing attention of many researchers on fundamental studies as well as industrial applications.[11–14]

The main drawback of BF is the lack of adhesion to many polymers, especially polyolefins. The hydrophilic nature of fiber surface results in a low interaction with hydrophobic polymers. Physical and chemical fiber surface treatments improve adhesion between the polymer and the surface of the fibers by reducing the polarity or changing polarity of the fiber surface.[15–18]

This paper reports a study of the influence of chemical surface treatment (alkaline and acetylation) on the morphology and structure of BF. Mechanical, thermal, rheological properties, morphology, and miscibility of the components of recycled polypropylene (RPP)/BF composites are also investigated.

Experimental

Materials

RPP was obtained by controllable multi-extrusion (five times) process sequences in our laboratory, with initial MFI of 16.2 g/10 min (230°C/2.16 kg). The compatibilizer OREVAC C100, was a maleic anhydride grafted polypropylene (MAPP), an experimental product provided by ARKEMA (France), with MFI of 10 g/min and MA content grafted of 1% (by weight). BF have an average length of 168 μm (100 tests) and an average width of 15 μm (100 tests); they are obtained by a mechanical separating method at the Polymer Center in Hanoi from bamboo culms of HOA BINH (VIETNAM). Scanning electron microscopy (SEM) micrograph of the BF is shown in Figure 1.

Fiber treatment procedure

Dewaxed BF were dried at 105°C in vacuum for 24 h to constant weight (m_1) and then immersed into sodium hydroxide solutions having different concentrations (0.05, 0.1, 0.2, 0.25, 0.5, and 1 M) for a desired time at room temperature. Alkali fibers were immersed in absolute ethanol and distilled water until neutral pH was obtained; then they were dried at 105°C under vacuum to constant weight (m_{al}). The weight percent loss (WPL) of BF was calculated from Equation (1):

$$\mathrm{WPL}\,(\%) = (m_1 - m_{al})/m_1 \times 100\%. \qquad (1)$$

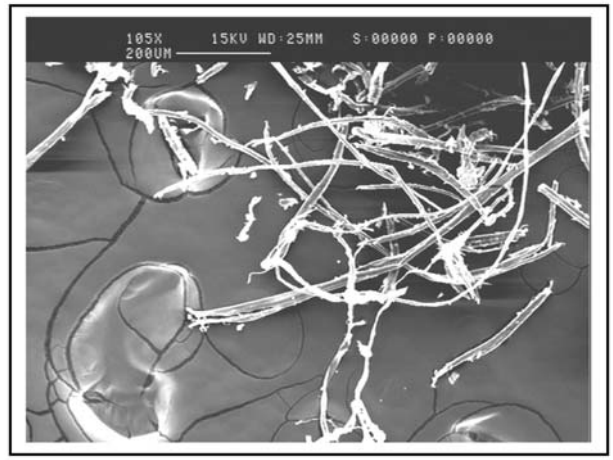

Figure 1. SEM micrograph of used BFs.

Dried alkali pretreated BF (m_2) were treated with pure acetic anhydride without catalyst at different temperatures (60°C, 70°C, 80°C, 90°C, and 100°C) for selected periods with respect to the ratio of fiber/anhydride solution of 1/15 by weight. Acetylated fibers were rinsed out in distilled water to remove residual acetic anhydride and acetic acid, and then dried at 105°C in vacuum to constant weight (m_{ac}). The weight percent gain (WPG) was calculated from Equation (2):

$$\mathrm{WPG}\,(\%) = (m_2 - m_{ac})/m_2 \times 100\%. \qquad (2)$$

Preparation of composites

RPP, compatibilizer, and BF were dried at 105°C in vacuum before melt blending in a co-rotating twin-screw extruder HAAKE with length-to-diameter ratio (L/D) 40 : 1 at temperature range from 175°C to 190°C. All samples were produced at the same screw speed (300 rpm). Extruded composite pellets were then added at 190°C to obtain specimens for determination of their mechanical properties. Table 1 shows appropriate nomenclatures and descriptions of different agro-composite formulations that were studied.

Mechanical properties characterization

Specimens have a parallelipedic shape of 78.9 × 9.8 × 4 mm with a notch angle of 45° and a 'V' notch depth of 0.4 mm. They were submitted to impact strength experiments. The test was carried out in impactmeter ZWICK machine according to the standard NF T51-035. At least five specimens were used for each test and the average value was reported.

Table 1. Nomenclature and description of composite samples

Key words	Description
RPP	Recycled PP, 5 times in extrusion
RPPBF20	Recycled PP, 20 wt% BF, without MAPP
RPPBF10MA10	Recycled PP, 10 wt% BF, 10 wt% MAPP
RPPBF20MA10	Recycled PP, 20 wt% BF, 10 wt% MAPP
RPPBF30MA10	Recycled PP, 30 wt% BF, 10 wt% MAPP
RPPBF40MA10	Recycled PP, 40 wt% BF, 10 wt% MAPP
RPPBF50MA10	Recycled PP, 50 wt% BF, 10 wt% MAPP
RPPAlBF20MA10	Recycled PP, 20 wt% alkali BF, 10 wt% MAPP
RPPAcBF20MA10	Recycled PP, 20 wt% acetylated BF, 10 wt% MAPP

In parallel, tensile tests were performed with dog-bone specimens on an INSTRON dynamometer choosing a cross-head speed of 50 mm/min and room temperature conditions according to the standard ISO EN527-2. At least five specimens were used for each test and the average value was reported.

Scanning electron microscopy

BF, cryogenic, and tensile fracture surfaces, after different treatments, were observed using scanning electron microscopy Stereoscan 240, Cambridge Instrument. All specimens were gold sputtered (about 40 μm) to avoid electrostatic charging and poor image resolution.

Infrared spectroscopy analysis

Changes in the structure of BF before and after chemical treatments were observed by Equinox 55 FTIR spectrometer (Sadis-Bruker Society) equipped with an ATR mono-reflexion. This instrument allowed analysis of fibers from the surface to a depth of 3 μm. Wavelength scanning ranges were taken from 400 to 4000 cm^{-1} with 128 points and at 4 cm^{-1} resolution.

Differential scanning calorimetry

Differential scanning calorimetry (DSC) analysis of RPP and of polymer composites samples were performed using a thermal analyzer PERKIN ELMER, Pyris 1. All measurements were made under N_2 flow (20 mL/min), keeping constant heating and cooling rates of 10°C/min. The analysis temperature was increased from 0°C to 200°C; about 5 mg of the sample was placed in an aluminum crucible of 40 μL volume, with a pinhole. In many cases, two tests were carried out to obtain reproducible results.

Viscoelastic properties measurement

We studied the rheological behavior of RPP/BF composites with different loadings of BF and compatibilizer content, using a laboratory rheometer Gemini 150 (Bohlin Instrument – England) under normal conditions. The dynamic measurements were carried out in a multiple frequency mode, over a range from 0.1 to 150 rad/s, using a cone-plan plate with a cone angle of 2.5° in oscillatory mode, at 190°C.

Results and discussion

Alkali treatment

Figure 2 compares SEM micrographs of BF treated in alkaline solution and fresh fibers. It shows that impurities on the surface of fibers were totally eliminated after treatment. Alkali treatment also created a change in topography of BF by the elimination of low weight molecules.

Natural fibers are mainly composed of cellulose, hemicellulose, and lignin. Hemicellulose contains several sugar molecules and some substances which are soluble in water or alkaline solutions. The structure of lignin is similar to that of unsaturated aromatic polymers and it may be soluble in an alkaline solution. Hemicellulose and lignin may partially dissolve during alkaline treatment, leading to a decreased mass of BF.

Figure 3(a) shows the influence of alkaline concentration on WPL of BF after 24 h at room temperature. These results indicated that the percentage of extracted components depended significantly on alkaline concentration: the greater the alkaline concentration, the higher the percentage loss of extracted components. WPL increases from 7.5% to 11.5% as alkaline concentration increases from 0.05 to 0.5 M before stabilizing (at greater concentrations).

Figure 3(b) shows the influence of alkali treatment time on WPL of BF. It was found that WPL values of BF increased significantly during the first 15 h of treatment and then began to stabilize after 24 h treatment.

Changes in the structure of the surface of BF were monitored by analyzing infrared spectra in mode ATR mono-reflexion (IR-ATR) as shown in Figure 4. It was observed that the surface structure of BF has changed during the treatment process. First, the peak at 3335.3 cm^{-1} assigned to stretching of hydroxyl group (–OH) and peak at 1030.3 cm^{-1} assigned to stretching of (–CO) groups in cellulose and hemicellulose were significantly reduced because of hemicellulose elimination. Secondly, the peak at 1621.9 cm^{-1}, corresponding to benzene ring stretching in lignin, decreased as the lignin was extracted. The peak at 1261.4 cm^{-1} assigned to acetyl stretching in lignin also decreased.

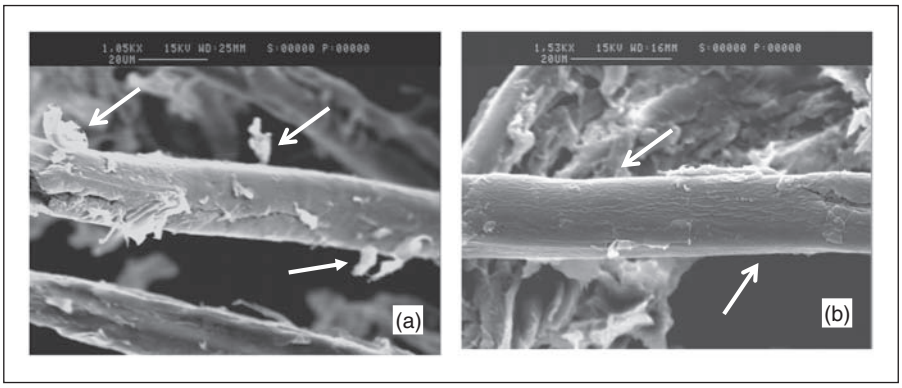

Figure 2. SEM micrographs of BFs (a) before; and (b) after alkali treatment.

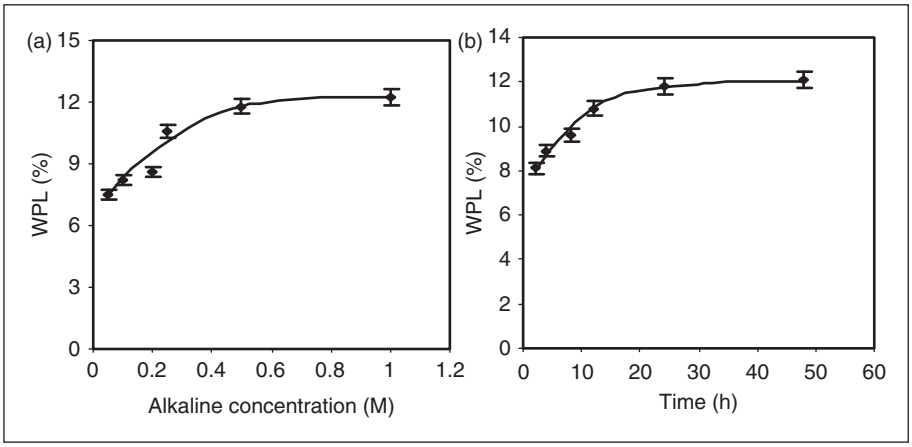

Figure 3. (a) Influence of alkaline concentration; and (b) treatment time with 0.5 M alkaline concentration on WPL of BFs.

Finally, vibrations corresponding to ($-CH_2$) and ($-CH_3$) stretching at 2915.4 cm^{-1} decreased after alkaline treatment. These results show that alkali treatment partially eliminates hemicellulose and lignin moieties in BF.

Acetylating treatment

In their natural state, BF are hygroscopic and have a tendency to reach equilibrium with atmospheric moisture. This property has restricted compatibility with most polymers, especially with polyolefins such as PE or PP, because their polarity and surface energies are significantly different.

To improve their compatibility with polymers, BF are often treated by chemical methods. Acetylation is one of the most effective methods to modify fiber surfaces. Its major aim is to reduce polarity by covering hydroxyl groups located on the cell wall of BF. Hydrogen atoms of hydroxyl groups are substituted by acetyl groups (esterification) as illustrated in Figure 5. During acetylation, WPG of fibers is proportional to the number of acetyl groups grafted onto the fiber surface because hydrogen atoms will be replaced by heavier acetyl groups. Depending on WPG during acetylation, we could estimate the efficiency of grafting.

As illustrated in Figure 6(a), WPG increases significantly with treatment time and starts to stabilize at 6 h before reaching a maximum WPG at about 9.4% after 10 h acetylation. Moreover, Figure 6(b) shows that WPG increases with increasing treatment temperature and raises WPG value by about 9.9% after 6 h at 100°C. This can be attributed to the fact that at higher temperatures and longer times, BF swell in the presence of acetic acid yielded during acetylation. More active sites will appear and so the reaction speed between BF and acetic anhydride is expected to be faster.

Structural change of fiber surfaces during acetylation is followed by determination of an infrared spectra in mode ATR mono-reflexion type (IR-ATR). Figure 7 presents ATR-IR spectrum of original and acetylated (6 h, 90°C) BF. Acetylation reduces the band peak intensities at 3422.1 and 1030.3 cm^{-1} corresponding to OH stretching. The intensity of the peaks at 1375.8 and 1245.3 cm^{-1} assigned to methyl group ($-CH_3$) stretching and acetyl stretching are greatly increased, due to the presence of acetyl groups in place of hydrogen

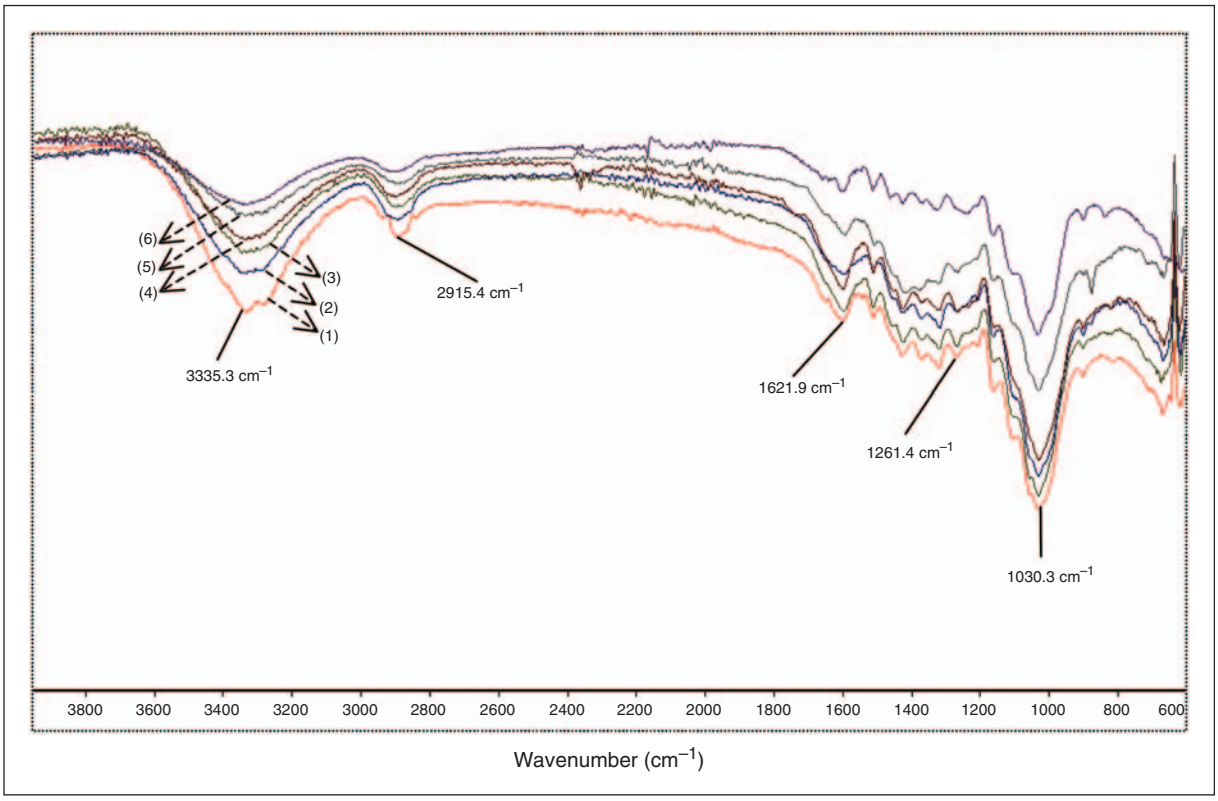

Figure 4. (1) IR-ATR spectrum of original BFs and alkali BFs with different concentration of NaOH; (2) 0.05 M; (3) 0.1 M; (4) 0.25 M; (5) 0.5 M; and (6) 1 M.

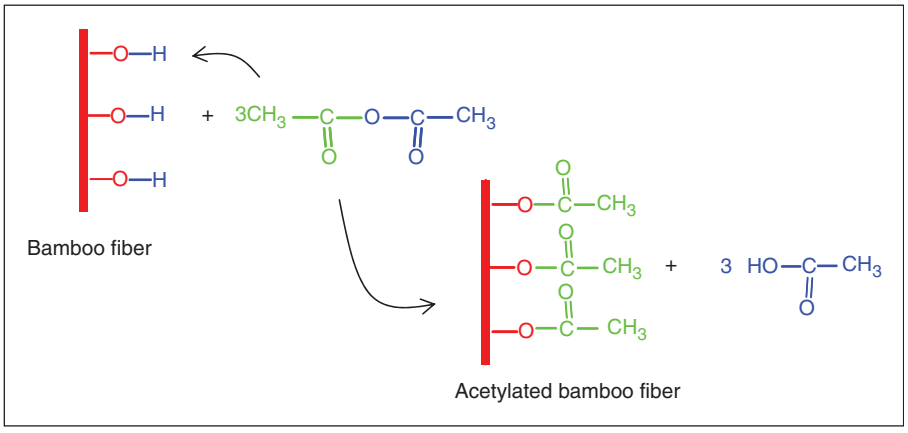

Figure 5. Mechanism proposed for acetylating reaction of BF using acetic anhydride.

atoms on the fiber cell wall. In addition, a new peak at 1735.4 cm^{-1} assigned to carbonyl (C=O) stretching of acetyl appears. ATR-IR spectra parameters allowed us to confirm the successful acetylation of our BF.

Mechanical properties of composites

Incorporation of a compatibilizer such as maleic anhydride grafted polypropylene (MAPP) into the formulation of RPP/BF composites improved the dispersion of BF in a RPP matrix, due to hydrogen bonding between the BF surface and the MAPP. In the present study, we added 10 wt% of MAPP in almost all formulations in order to enhance adhesion between the components. Table 2 shows the variations of mechanical properties of virgin polypropylene (PP), a recycled one (RPP), and composites depending on fiber content and treatment methods. A slight diminution of tensile strength in comparison with RPP was observed at a low fiber content (20 wt%). Composites exhibited better tensile strength

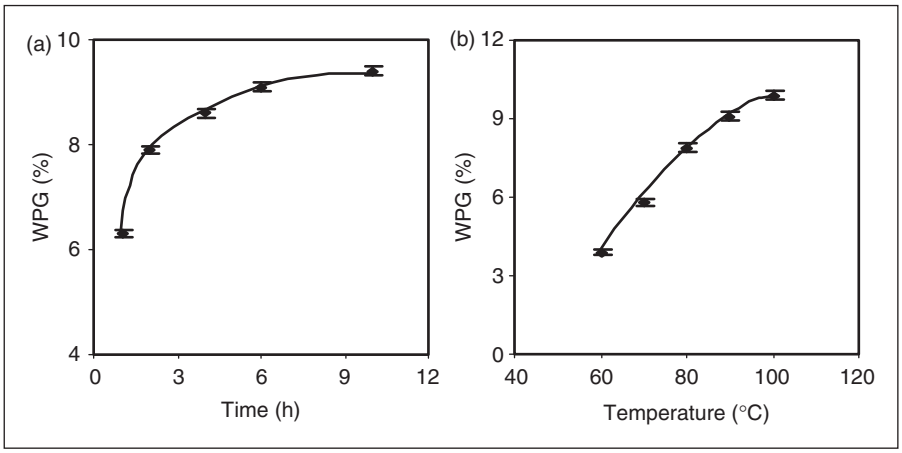

Figure 6. (a) Effect of treatment time at 90°C; and (b) temperature acetylation during 6 h on WPG of BFs.

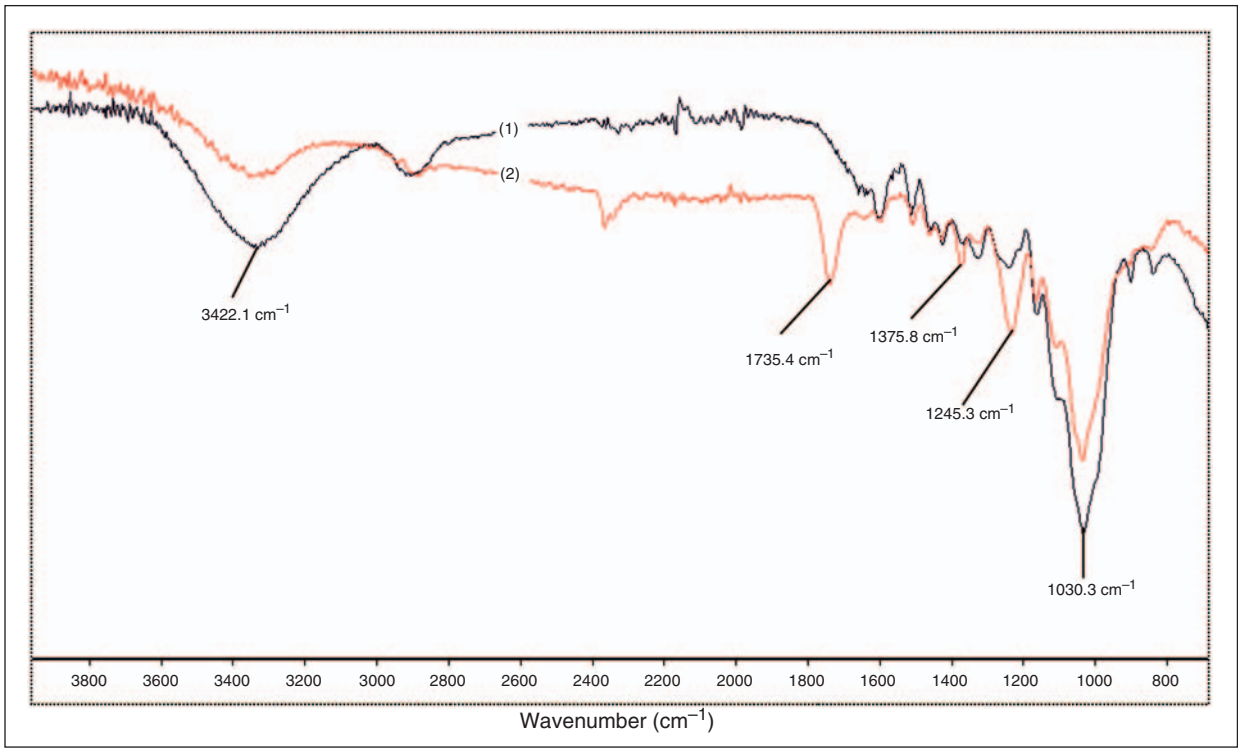

Figure 7. (1) IR-ATR spectrum of original; and (2) acetylated BFs.

than RPP with further addition of BF, and reached a maximum value around 29 MPa for 40 wt% FB content sample; this value seemed to stabilize at higher fiber loading (50 wt%).

Charpy impact strength increases with increasing the fiber loadings from 10 to 40 wt% and reached a value of 3.7 kJ/m^2 (40 wt%), which is 32% higher than the RPP one. However, the addition of more fiber (50 wt%) did not increase Charpy impact strength. Alkali and acetylated BF enhanced tensile strength of composites compared with untreated samples. Alkali and acetylated fiber-reinforced RPP led to an increase of 23% and 35% Charpy impact strength compared with untreated samples. Tensile strength increased 12% and 29% after such treatment. Composite samples reinforced with original BF without compatibilizer had less favorable mechanical properties. These results showed that RPP compatibilized with MAPP reinforced by acetylated BF exhibited the best mechanical properties.

Fractured surface

Figure 8 shows SEM micrographs of composites based on BF-RPP, containing 20 wt% fiber loading.

The micrograph (Figure 8(a)) of composites reinforced with original BF without compatibilizer shows very poor adhesion between original BF surface and matrix. There are many large void spaces enclosed in the BF and the fibers lack contact with matrix because of the incompatibility of these components. This can explain the poor mechanical properties of these composites. Addition of MAPP (Figure 8(b)) led to a slightly enhanced composite adhesion and reduced interface distance between the two phases; but some hollow slots in the interfaces between BF and RPP were still observed. Alkali treatment increased dimensional stability and surface roughness of BF and thus improved the adhesion with RPP (Figure 8(c)). We also observed that BF were partially wetted by the matrix.

In the case of composites reinforced by acetylated BF, a homogeneous dispersion of BF in the matrix with few voids in the surface was observed; acetylated BF tended to remain in the matrix rather than to detach after tensile tests. This was due to the strong adhesion of these components. The fibers were totally wetted by matrix polymer (Figure 8(d)).

Table 2. Mechanical properties of RPP/BF composites

Sample	Tensile strength (MPa)	Charpy strength (kJ/m^2)
PP	32.4 ± 0.7	4.4 ± 0.2
RPP	25.4 ± 0.4	2.8 ± 0.2
RPPBF20	22.4 ± 0.3	2.4 ± 0.2
RPPBF10MA10	25.3 ± 0.3	2.8 ± 0.2
RPPBF20MA10	26.5 ± 0.4	3.1 ± 0.2
RPPBF30MA10	27.4 ± 0.6	3.3 ± 0.2
RPPBF40MA10	29.2 ± 0.3	3.7 ± 0.2
RPPBF50MA10	28.6 ± 0.2	3.6 ± 0.2
RPPAlBF20MA10	29.7 ± 0.1	3.8 ± 0.2
RPPAcBF20MA10	31.6 ± 0.3	4.2 ± 0.2

Note: AlBF is alkali bamboo fiber; AcBF is acetylated bamboo fiber; and MA is maleic anhydride grafted polypropylene.

Thermal properties

The effect of BF on thermal properties of RPP was investigated using DSC technique. All crystallization, melting temperatures, and enthalpies (T_c, T_m, ΔH_c, ΔH_m) obtained by DSC scans are summarized in Table 3. The normalized crystallization percentage (X_c) was determined using the classical Equation (3):

$$X\% = (\Delta H_c/\Delta H_{100}) \times 100\%, \qquad (3)$$

where X is the crystallization percentage, ΔH_c the enthalpy of the analyzed sample (J/g) and ΔH_{100} the enthalpy corresponding to the standard thermal crystallization value of 100% crystalline polymer sample. In the case of PP, the ΔH_{100} value is 209 J/g.[19]

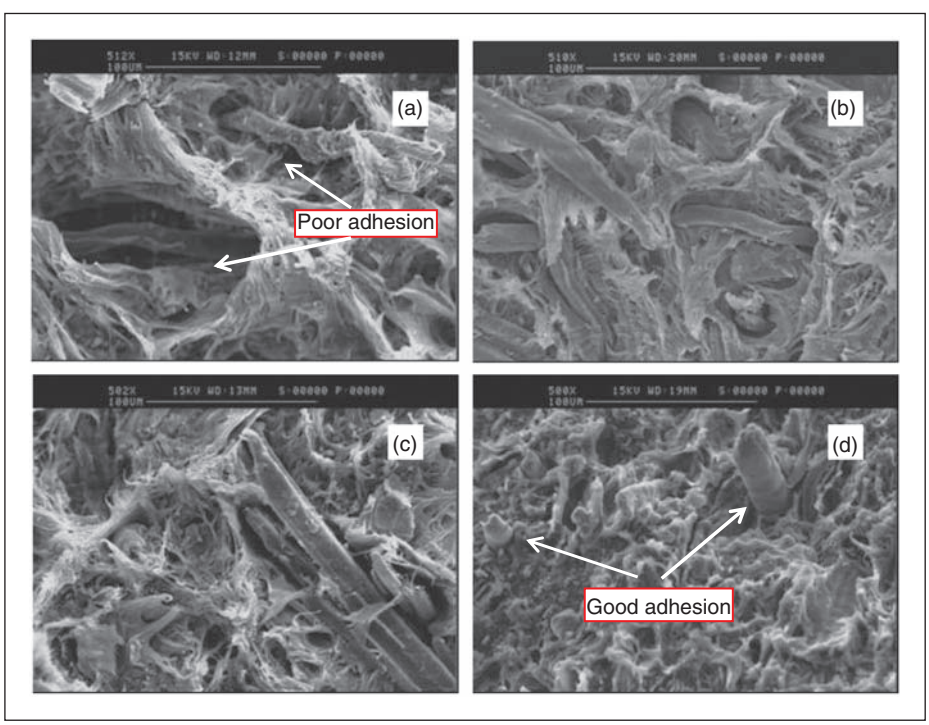

Figure 8. SEM micrographs of different BFs reinforced recycled polypropylene composites samples: RPPBF20 (a); RPPBF20MA10 (b); RPPAlBF20MA10 (c); and RPPAcBF20MA10 (d).

Table 3 shows that the $T_{m\text{-MAPP}}$ remained almost constant, independently of fiber content, even in the case of composites reinforced with chemically treated BF. Melt temperature peaks of RPP in composites slightly decreased (Table 3). This might be explained by the presence of BF in the RPP matrix. BF may disturb the crystallization process of the matrix by decreasing the organization of the spherulites and initiating a transcrystallization process at the bamboo/matrix interface.

Generally, the introduction of fibers increased both crystallization rate and crystalline percentage of RPP whatever the loading rates.[20–22] The crystallization percentage increased significantly (14.6% with RPPBF10MA10 sample) in the presence of BF in PP matrix and the increment reached 21.4% when 50 wt% BF were added to the formulation. In all fiber loadings studied, the non-isothermal crystallization of recycled resins in the composites occurs at higher temperatures than that of pure RPP, indicating that the BF accelerated this process. This can be explained by the 'nucleation agent effect' of BF inside the polymer matrix that provides more nucleation sites in RPP and also increases the crystallization rate of RPP.[23,24]

Rheological properties

In general, neat polymers exhibit linear viscoelastic behavior in the low strain region, in which the storage modulus (G') and loss modulus (G'') are independent of the applied strain. But in the case of composite materials, viscoelastic behavior depends strongly on the nature of the polymer and interactions between its components (reinforcements–reinforcements, polymer–reinforcements, compatibilizer–reinforcements). The increase of reinforcement rates in the formulation generally leads to reduction or even disappearance of viscoelastic behavior of composites, because the interaction's reinforcements–reinforcements become more important.

Plots of normalized modulus values as a function of strain were used to determine the linear viscoelastic region of RPP and their composite. Figure 9 shows the evolution of normalized modulus ($G'\omega/G'\omega_0$) depending on the applied strain at 190°C with a frequency of 10 rad/s for RPP and composites containing 50% BF. We observed a 'plateau region' corresponding to the viscoelastic behavior of materials when the strain was below a critical value (ω_c).

When the applied strain exceeds the critical value ω_c the modulus decreases with increasing of strain. This phenomenon, named 'Payne' effect[25] appears when the plateau region clearly changes its slope. The value of the critical strain for the composite was about 7%, four times lower than that of RPP (30%). To ensure that all tests would be performed in the linear zone (Newtonian zone), we decided to work at a fixed strain of 1% for all measurements in frequency scanning.

Figure 10 shows the evolution of G' and η^* as a function of frequency at different BF contents (10–50 wt%). We saw clearly that the presence of BF and

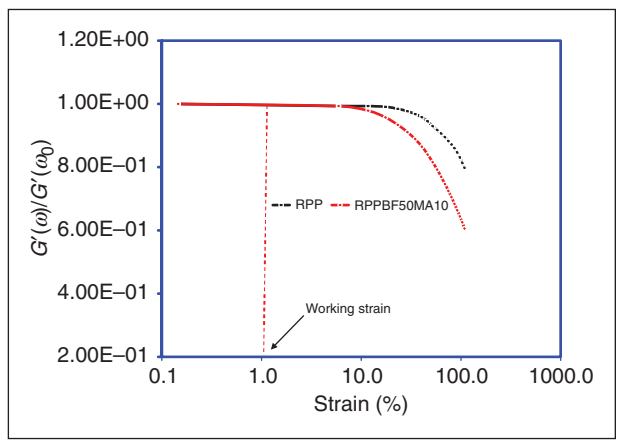

Figure 9. Determination of dynamic linear region of RPP and composite containing 50 wt% BF ($\omega_0 = 0.1\%$; dynamic frequency = 5 rad/s; $T = 190°C$).

Table 3. Thermal properties of RPP/BF composites

Sample	$T_{m\text{-MAPP}}$ (°C)	$\Delta H_{m\text{-MAPP}}$ (J/g)	$T_{m\text{-RPP}}$ (°C)	$\Delta H_{m\text{-RPP}}$ (J/g)	T_c (°C)	X_c (%)
MAPP	130.64	37.6	–	–	117.3	58.1
RPP	–	–	166.6	88.7	115.5	45.6
RPPBF10MA10	127.89	10.8	165.9	74.5	116.8	52.3
RPPBF20MA10	127.34	12.2	165.4	68.9	117.4	53.5
RPPBF30MA10	127.79	11.9	165.1	59.1	117.9	54.1
RPPBF50MA10	127.67	12.0	165.1	53.9	118.3	55.4
RPPAlBF20MA10	128.01	9.9	165.2	65.6	117.3	60.5
RPPAcBF20MA10	128.34	9.4	165.7	67.4	117.6	61.5

compatibilization significantly influenced the rheological properties of the system. The addition of BF in the RPP matrix increased their complex viscosity (η^*), especially at low dynamical frequency. Indeed, interactions between BF and compatibilizer resulted in increased viscosity of the composite, even though the compatibilizer viscosity (PP grafted) was much lower than that of virgin PP. In addition, the presence of BF in the composite may hinder movements of polymer chains during flow and so increase the viscosity of the material. We found that the complex viscosity increased sharply with increase of BF content in the composite.

We noted that the G' and G'' values for the composites were higher than those corresponding to neat PP in the whole frequency zone studied (Figures 10 and 11). These values are proportional to BF content of the formulation. According to Tian et al.,[26] the modules G' and G'' of linear polymers at the terminal zone (low frequency) are proportional to the frequencies by the well-known relations: G'–ω^2 and G''–ω. However, the slopes of G' and G'' for the composites decreased greatly with the increase of BF content, and these values were smaller than those obtained for neat RPP. This may be attributed to the fact that the relaxation time of polymer chains in the composite is higher than that of neat PP and so there may be some longer relaxation processes. The extension of relaxation time in the terminal zone (low frequency) for composites is usually due to poor compatibility between components and the presence of solid phase in the polymer matrix.[27]

The flow behavior of neat polymers depends mainly on the geometry of the flow and processing conditions. In the case of composites, the flow behavior is more complex because of interactions of their components. When the frequency (ω) of the applied strain is low (long time), the flow behavior of the composite is similar to that of a viscous material, and conversely, if the frequency (ω) is high (short time), the polymer shows an elastic-like behavior. The transition of viscoelastic states named 'transitional point' can be determined, quite simply, when the value of tangent (δ) is equal to 1 (tangent $= G''/G'$). The plastic absolute materials possess an infinite tangent (δ) value (∞) and, contrary, elastic materials have a tangent value nearly to zero.[28] Thus, the higher the tangent (δ) value, the less elastic behavior the material exhibits. Figure 11 shows that the tangent values decrease with increasing of BF content in the whole frequency zone studied. Tangent values (δ) of neat RPP decreased monotonically with increasing frequency and were always greater than one, which means there is no 'transitional step' when neat PP changes from a viscous state to the elastic state. We observed a sharp decrease of tgδ with increasing BF content from 40% to 50% in weight at low frequency (0.01 rad/s). This can be explained by the existence of a critical value of the 'concentration' (concentration of percolation) of BF in the composite. When BF contents are higher than those of the critical concentration value, BF may tend to form agglomerates which increase interaction forces between the BF.[29]

Indeed, at low frequency, the value of storage modulus for composite (G'_{com}) is the sum of several module constituents[30]:

$$G'_{com} = G'_{RPP} + G'_{det} + G'_{inter}, \quad (4)$$

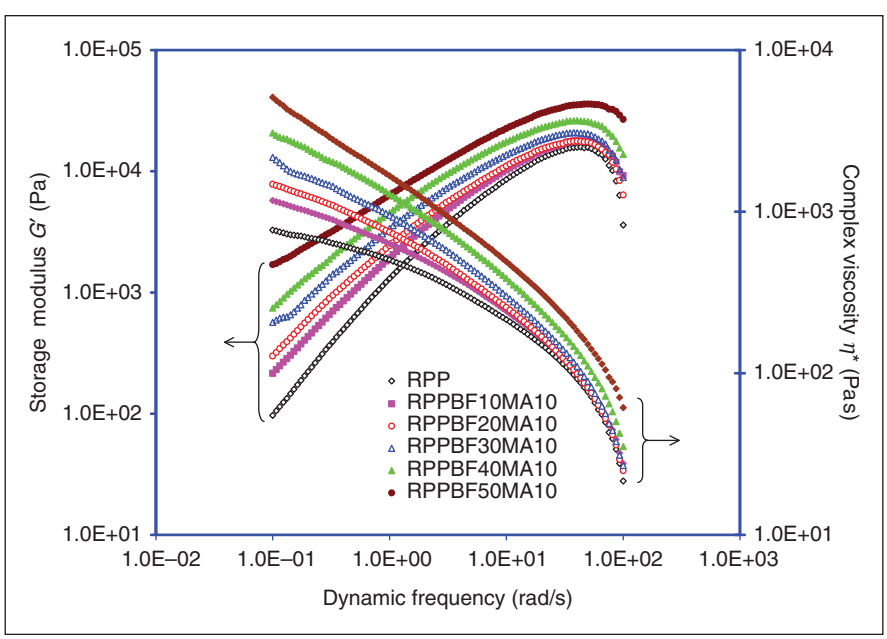

Figure 10. Storage modulus and complex viscosity of composites at different BF content as a function of dynamic frequency.

where G'_{RPP} is the storage modulus of the RPP matrix, G'_{det} is the storage modulus corresponding to the detention process and G'_{inter} is the storage modulus corresponding to the interactions between the BF. When the BF content exceeds the critical value, G'_{inter} becomes very high compared to other modulus due to friction between agglomerates which leads to a significant increase of G'_{com}.

A very interesting method developed by Cole–Cole justifies the miscibility of the components in composites by using the rheological data.[31,32] Indeed, by plotting η'' values as a function of η' values (Figure 12), we can

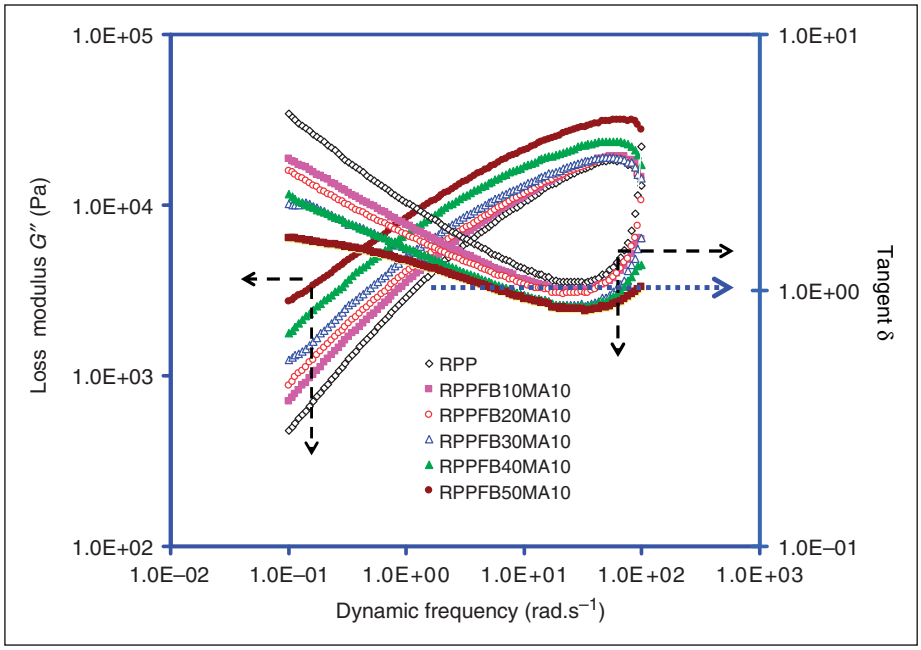

Figure 11. Loss modulus and tangent δ of composites at different BF content as a function of dynamic frequency.

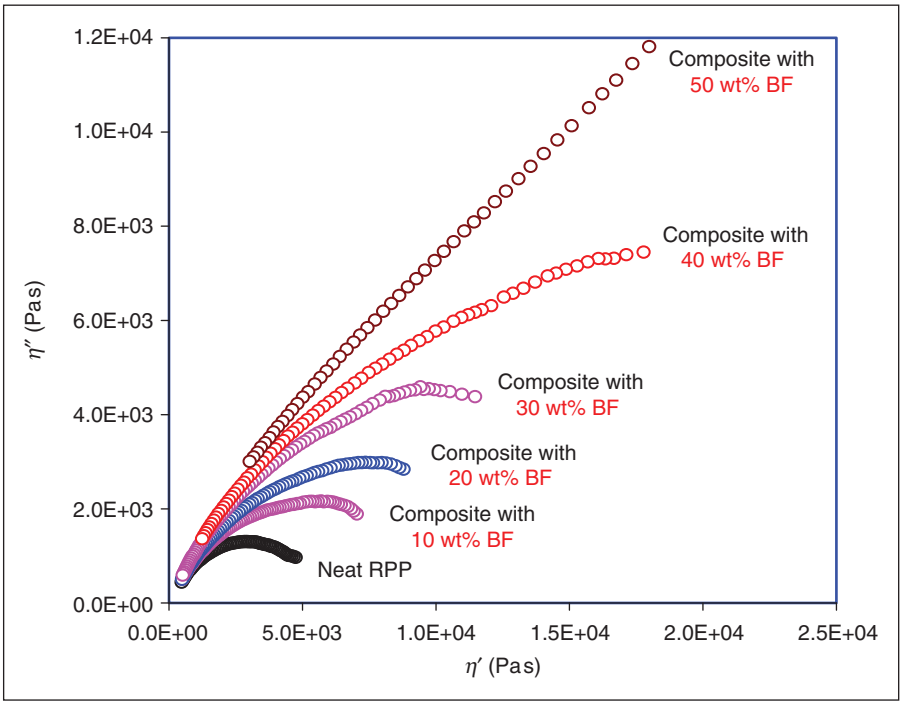

Figure 12. Plotting η'' vs. η' of composite at different BF content using Cole–Cole method.

evaluate the miscibility of these components by observing the form of the curves obtained. If the composite is miscible and homogeneous, the curves (η''–η') plotted are quite smooth and resemble a semicircle curve plotting η'' values as a function of η' values for RPP and their composites at different BF contents. We note that the shape of the curve corresponding to neat PP recycled presents a perfect 'semicircle' because there is only a phase of pure polymer in this case. When we add BF to the formulation, the curves become irregular and more open. In particular, when the BF percentage in the composite exceeds 40% (in weight), the curve becomes linear, reflecting poor uniformity and compatibility between components in the composite. These results are in agreement with SEM observations showing the appearance of agglomerates from 40 wt% in weigh BF (Figure 14).

Figure 13 shows the influence of fiber treatment methods on the miscibility of the composites prepared with the same content of BF (20 wt%). It shows that the

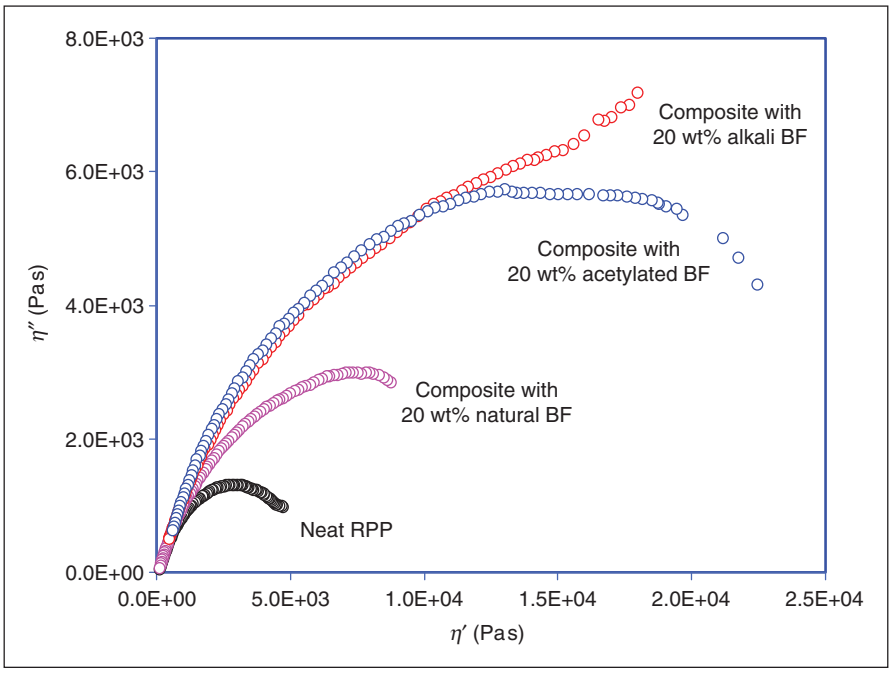

Figure 13. Plotting η'' vs. η' of composite reinforced by natural and chemically treated bamboo fibers using Cole–Cole method.

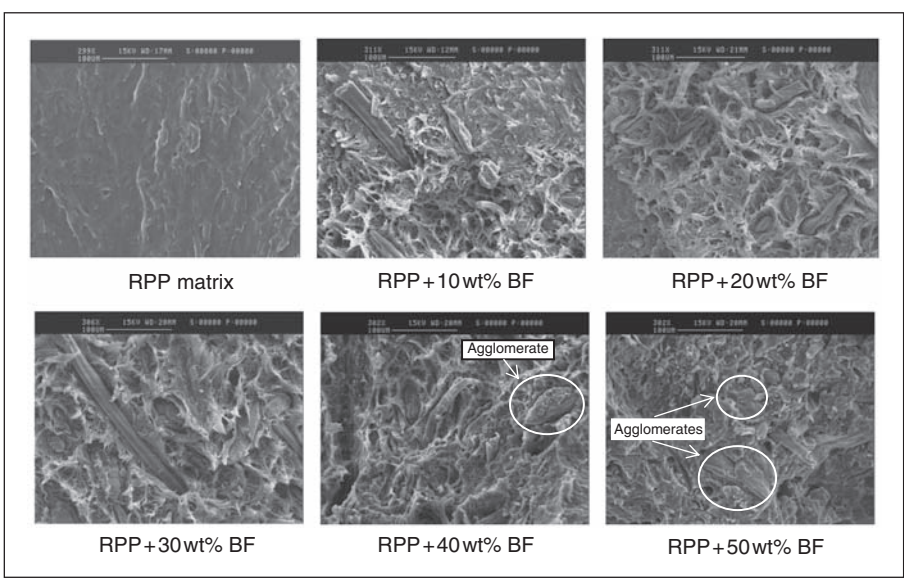

Figure 14. SEM micrographs of RPP/BF composites at different BFs loading.

chemical treatments of BF (alkali and acetylation) lead to more open curves with higher η' and η'' values compared with those of untreated BF. This is because the treatments increase modules G' and G'' composite compared to composites reinforced by untreated BF. We also observed, as shown in Figure 13, that treatment with sodium hydroxide decreased the miscibility of the composite since the (η''–η') curve of the composite has a fairly complex shape with many deviation points. On the contrary, acetylation of BF led to smoother curves, indicating an improvement of miscibility of components in the formulation.

Conclusions

The influence of treatment conditions on BF surfaces by sodium hydroxide alone (alkaline) or by acetylation has been studied. The WPL depends on treatment times and on sodium hydroxide concentration. The sodium hydroxide concentration may be decreased by an increase in treatment time. The efficiency of acetylating reactions was also investigated by measuring WPG and by analyzing IR-ATR parameters.

Effects of specific conditions of alkali treatment or both alkali and acetylation treatments on mechanical properties (tensile and Charpy impact strength) were investigated. The mechanical properties of RPP composites reinforced by BF slightly increased after treatment with an alkaline solution. Mechanical properties of composites were improved when reinforced by acetylated BF. SEM showed that adhesion improved at the interface between BF surface and matrix PP after alkali and acetylation treatments. Incorporation of MAPP compatibilizer led to better adhesion between BF and RPP matrix. The presence of BF in composite formulation slightly decreased the melting temperature of the matrix and increased crystallization percentage. The presence of BF increased both storage modulus and loss modulus of RPP/BF composites. Chemical treatments of BF led to more open curves with higher η' and η'' values compared with those of untreated BF.

Acknowledgments

The first author would like to thank Prof. Jack R. Plimmer from the Agricultural Research Service, U.S.D.A, Beltsville, USA for his fine discussion during this work. The authors are also grateful to the Vietnamese Government for financial supports (grant number QD/CP322) for this work.

References

1. Eichhorn SJ, Baillie CA, Zafeiropoulos N, Mwaikambo LY, Ansell MP, Dufresne A, et al. Review: current international research in cellulosic fibers and composites. *J Mater Sci* 2001; 36: 2107–2131.
2. Raj RG, Kokta BV and Daneault C. Wood flour as a low-cost reinforcing filler for polyethylene: studies on mechanical properties. *J Mater Sci* 1990; 25: 1851–1855.
3. David H and Michael W. Interaction between coupling agent and lubricants in wood-polypropylene composites. *Compos Part A: Appl Sci Manuf* 2004; 35: 385–394.
4. Ibon AA, Thomas L and Alexander B. Wetting behavior of flax fibers as reinforcement for polypropylene. *J Coll Inter Sci* 2003; 263: 580–589.
5. Ajay K, Chauhan SS, Jayant MM and Manas C. Mechanical properties of wood–fiber reinforced polypropylene composites: effect of a novel compatibilizer with isocyanate functional group. *Compos Part A: Appl Sci Manuf* 2007; 38: 227–233.
6. Naik JB and Mishra S. Esterification effect of maleic anhydride on surface and volume resistivity of natural fiber/polystyrene composites. *Polym Plast Technol Eng* 2007; 46: 537–540.
7. Sy Trek S. Composites from newsprint fiber and polystyrene. *Polym Plast Technol Eng* 2007; 46: 421–425.
8. Keener TJ, Stuart RK and Brown TK. Maleated coupling agents for natural fiber composites. *Compos Part A: Appl Sci Manuf* 2004; 35: 357–363.
9. Haihong J and Pascal KD. Development of poly(vinyl chloride)/wood composites. A literature review. *J Vinyl Add Tech* 2004; 10: 59–69.
10. Albermani F. Review: an apparatus for interconnecting structural elements. World Intellectual Property Organization Patent, WO/2008/009054.
11. Yongli M, Xiaoya C and Qipeng G. Bamboo fiber-reinforced polypropylene composites: crystallization and interfacial morphology. *J Appl Polym Sci* 1997; 64: 1267–1273.
12. Xiaoya C, Qipeng G and Yongli M. Bamboo fiber-reinforced polypropylene composites: A study of mechanical properties. *J Appl Polym Sci* 1998; 69: 1891–1899.
13. Murali Mohan RK. Extraction of tensile properties of natural fibers: vakka, date and bamboo. *Compos Struct* 2007; 77: 288–295.
14. Mahuya D and Debabrata C. Influence of mercerization on the dynamic mechanical properties of bamboo, a natural lignocellulosic composite. *Indus Eng Chem Res* 2006; 45: 6489–6492.
15. Xue L, Lope G and Satyanarayan P. Chemical treatments of natural fiber for use in natural fiber-reinforced composites: a review. *J Polym Environ* 2007; 15: 25–33.
16. Nabi SD and Jog JP. Natural fiber polymer composites: a review. *Adv Polym Tech* 1999; 18: 351–363.
17. Paul W, Jan I and Ignaas V. Natural fibers: can they replace glass in fiber reinforced plastics? *Compos Sci Technol* 2003; 63: 1259–1264.
18. Bledzki AK and Gassan J. Composites reinforced with cellulose based fibers. *Prog Polym Sci* 1999; 24: 221–274.
19. Zafeiropoulos NE, Williams DR, Baillie CA and Matthews FL. Engineering and characterization of the interface in flax fiber/polypropylene composite materials. Part I. Development and investigation of surface treatments. *Compos Part A* 2002; 33: 1083–1093.

20. Yao F, Wu Q, Lei Y and Xu Y. Rice straw fiber-reinforced high-density polyethylene composite: effect of fiber type and loading. *Indus Crops Prod* 2008; 28: 63–72.
21. Somnuk U, Eder G, Phinyocheep P, Suppakarn N, Sutapun W and Ruksakulpiwa Y. Quiescent crystallization of natural fibers-polypropylene composites. *J Appl Polym Sci* 2007; 106: 2997–3006.
22. Sameni UJK, Ahmad SH and Zakaria S. Performance of rubberwood fiber-thermoplastic natural rubber composites. *Polym Plast Tech Eng* 2003; 42: 139–152.
23. Singh S, Mohanty AK, Sugie T, Takai Y and Hamada H. Renewable resource based biocomposites from natural fiber and polyhydroxybutyrate-co-valerate (PHBV) bioplastic. *Compos Part A: Appl Sci Manuf* 2008; 39: 875–886.
24. Beg MDH and Pickering KL. Fiber pretreatment and its effects on wood fiber reinforced polypropylene composites. *Mater Manuf Proc* 2006; 21: 303–307.
25. Payne AR and Whittaker R. Low strain dynamic properties of filled rubbers. *Rubber Chem Tech* 1971; 44: 440–478.
26. Tian JH, Yu W and Zhou CX. The preparation and rheology characterization of long chain branching polypropylene. *Polymer* 2006; 47: 7962–7969.
27. Utracki LA and Sammut P. Rheological evaluation of polystyrene-polyethylene blends. *Polym Eng Sci* 1988; 28: 1405–1415.
28. Limei C, Zhen Z, Yong Z, Inxi YZ, Xiangfu Z and Wen Z. Rheological behavior of polypropylene/novolac blends. *J Appl Polym Sci* 2007; 106: 811–816.
29. Hong-Mei Y, Qiang Z and Miao D. Rheological behavior of the melts for polyethylene-based montmorillonite nanocomposites. *Chem Res Chin Univ* 2006; 22: 651–657.
30. Jian L, Cixing Z, Gang W and Delu Z. Study on rheological behavior of polypropylene/clay nanocomposites. *J Appl Polym Sci* 2003; 89: 3609–3617.
31. Cole KS and Cole RH. Dispersion and absorption in dielectrics. I. Alternating current characteristics. *J Chem Phys* 1941; 9: 341–351.
32. Joshi M, Butola BS, Simon G and Kukaleva N. Rheological and viscoelastic behavior of HDPE/cctamethyl-POSS nanocomposites. *Macromolecules* 2006; 39: 1839–1849.